AGU PUBLICATIONS

Global Biogeochemical Cycles

RESEARCH ARTICLE
10.1002/2015GB005106

Key Points:
- New observational constraints on the ocean atmosphere ammonia flux
- Ocean NH_3 flux to the atmosphere is lower than previous estimates
- Photolysis of organic N may contribute to the release of N from the ocean

Supporting Information:
- Figure S1
- Figure S2
- Figure S3
- Figures S1–S3

Correspondence to:
F. Paulot,
Fabien.Paulot@noaa.gov

Citation:
Paulot, F., D. J. Jacob, M. T. Johnson, T. G. Bell, A. R. Baker, W. C. Keene, I. D. Lima, S. C. Doney, and C. A. Stock (2015), Global oceanic emission of ammonia: Constraints from seawater and atmospheric observations, *Global Biogeochem. Cycles*, *29*, 1165–1178, doi:10.1002/2015GB005106.

Received 28 JAN 2015
Accepted 14 JUL 2015
Accepted article online 17 JUL 2015
Published online 13 AUG 2015

Global oceanic emission of ammonia: Constraints from seawater and atmospheric observations

F. Paulot[1,2,3], D. J. Jacob[3], M. T. Johnson[4,5], T. G. Bell[6], A. R. Baker[7], W. C. Keene[8], I. D. Lima[9], S. C. Doney[9], and C. A. Stock[2]

[1]Program in Atmospheric and Oceanic Sciences, Princeton University, Princeton, New Jersey, USA, [2]Geophysical Fluid Dynamics Laboratory/National Oceanic and Atmospheric Administration, Princeton, New Jersey, USA, [3]School of Engineering and Applied Sciences, Harvard University, Cambridge, Massachusetts, USA, [4]Centre for Ocean and Atmospheric Science, University of East Anglia, Norwich, UK, [5]Center for Environment, Fisheries, and Aquaculture Science, Lowestoft, UK, [6]Plymouth Marine Laboratory, Plymouth, UK, [7]School of Environmental Sciences, University of East Anglia, Norwich, UK, [8]Department of Environmental Sciences, University of Virginia, Charlottesville, Virginia, USA, [9]Department of Marine Chemistry and Geochemistry, Woods Hole Oceanographic Institution, Woods Hole, Massachusetts, USA

Abstract Current global inventories of ammonia emissions identify the ocean as the largest natural source. This source depends on seawater pH, temperature, and the concentration of total seawater ammonia (NH_x(sw)), which reflects a balance between remineralization of organic matter, uptake by plankton, and nitrification. Here we compare [NH_x(sw)] from two global ocean biogeochemical models (BEC and COBALT) against extensive ocean observations. Simulated [NH_x(sw)] are generally biased high. Improved simulation can be achieved in COBALT by increasing the plankton affinity for NH_x within observed ranges. The resulting global ocean emissions is 2.5 TgN a^{-1}, much lower than current literature values (7–23 TgN a^{-1}), including the widely used Global Emissions InitiAtive (GEIA) inventory (8 TgN a^{-1}). Such a weak ocean source implies that continental sources contribute more than half of atmospheric NH_x over most of the ocean in the Northern Hemisphere. Ammonia emitted from oceanic sources is insufficient to neutralize sulfate aerosol acidity, consistent with observations. There is evidence over the Equatorial Pacific for a missing source of atmospheric ammonia that could be due to photolysis of marine organic nitrogen at the ocean surface or in the atmosphere. Accommodating this possible missing source yields a global ocean emission of ammonia in the range 2–5 TgN a^{-1}, comparable in magnitude to other natural sources from open fires and soils.

1. Introduction

Anthropogenic nitrogen fixation is estimated to contribute over 50% of present-day global nitrogen fixation [*Fowler et al.*, 2013]. One of the consequences of greater anthropogenic nitrogen fixation is an increase of ammonia (NH_3) emissions to the atmosphere, with recent estimates suggesting that anthropogenic sources, primarily agriculture, account for over 70% of global NH_3 emissions (65 TgN a^{-1}) [*Sutton et al.*, 2013]. Quantifying the implications of this increase for air quality or nitrogen deposition depends in part on our knowledge of natural sources. Previous studies suggest that the ocean is the largest natural source of NH_3 to the atmosphere, accounting for over 40% of all natural NH_3 emissions (Table 1) and 15% of global NH_3 emissions [*Bouwman et al.*, 1997; *Paulot et al.*, 2014].

Observations have shown that the ocean could act as a net source of NH_3 to the atmosphere locally [*Quinn et al.*, 1992, 1996; *Gibb et al.*, 1999; *Jickells et al.*, 2003; *Johnson et al.*, 2008] depending on the concentration of NH_3 in seawater ($NH_x(sw) \equiv NH_3(sw) + NH_4^+(sw)$) as well as physical parameters such as temperature, pH, and salinity [*Bouwman et al.*, 1997; *Johnson et al.*, 2008]. [NH_x(sw)] is generally low relative to other dissolved nitrogen species [*Gruber*, 2008], and to our knowledge, no global survey exists unlike for other nutrients [e.g., *Garcia et al.*, 2014]. As a result, the magnitude of global oceanic NH_3 emissions remains highly uncertain (Table 1).

A large marine source of NH_3 could exert an important influence on the pH of marine aerosols by neutralizing sulfuric acid produced from atmospheric oxidation of marine dimethylsulfide (DMS). NH_3 has also been shown to lower the vapor pressure of sulfuric acid and may thus contribute to new particle formation in the marine atmosphere [*Ball et al.*, 1999; *Berndt et al.*, 2010; *Benson et al.*, 2011; *Zhang et al.*, 2011; *Almeida et al.*, 2013],

Table 1. Present-Day Natural NH_3 Emissions[a]

	Ocean	Open Fires	Natural Soils	Wildlife	Volcanoes	Total
Clarke and Porter [1993]	23	-	-	-	-	-
Schlesinger and Hartley [1992]	13	5	10	-	-	28
Dentener and Crutzen [1994]	7	-	5.1	2.5	-	20.5[b]
Bouwman et al. [1997]	8.2	5.9	2.4	0.1	-	16.5
Sutton et al. [2013]	8.2	5	2.4	2.5	0.4	18.5
This work	2–5	3.5	2.4	0.3	0.9	9.5–12.5

[a]TgN a^{-1}. Anthropogenic emissions in our work are 38 TgN a^{-1} and 30–46 TgN a^{-1} in the literature [*Paulot et al.*, 2014; *Sutton et al.*, 2013]. Ocean and soils are gross sources, not accounting for atmospheric deposition.
[b]Adding 5 TgN a^{-1} from open fires.

although the growth of clusters may be inhibited by the large surface area of primary marine aerosol over the ocean [*Quinn and Bates*, 2011].

Here we use simulated monthly concentrations of NH_x(sw) from two ocean biogeochemistry models (BEC) [*Moore et al.*, 2001, 2004] and (COBALT) [*Stock et al.*, 2014a] to simulate ocean emissions of ammonia in a global atmospheric chemistry model (GEOS-Chem). We use both seawater and atmospheric observations to evaluate the simulations and derive an estimate of the ocean source of ammonia to the atmosphere.

2. Observations

We use observations of atmospheric NH_4^+, Cl^-, Na^+, SO_4^{2-} aerosols, NH_3 gas, and seawater NH_x collected over the last 20 years (Table 2). Atmospheric NH_4^+ observations provide better spatial coverage than NH_x(sw) and gas phase NH_3, especially in the Atlantic Ocean, which has been extensively sampled by the Atlantic Meridional Transect (AMT) program [*Aiken and Bale*, 2000]. NH_4^+, SO_4^{2-}, Cl^-, and Na^+ aerosol observations were collected by cyclonic filter packs [*Quinn et al.*, 1988] and cascade impactors [*Keene et al.*, 2009; *Baker et al.*, 2010]. NH_3 was measured using filter packs [*Johnson et al.*, 2008] or mist chambers [*Keene et al.*, 1989]. NH_x(sw) observations originate primarily from intensive campaigns, such as the U.S. Joint Global Flux Study (http://usjgofs.whoi.edu/), which have limited spatial coverage but sample the main ocean biomes. Depending on the technique used, (Berthelot reaction [*Solorzano et al.*, 1969; *Whitledge et al.*, 1981], orthopthaldealdehyde fluorimetry [*Holmes et al.*, 2001], flow injection ion chromatography [*Gibb et al.*, 1999]), detection limits vary from 0.002 to 0.08 mmol m^{-3}.

3. Methods

Here we describe the simulation of oceanic ammonia in GEOS-Chem including the representation of NH_x(sw) sources and sinks in BEC and COBALT, the parameterization of the exchange of NH_3 between ocean and atmosphere, and the processes controlling the atmospheric budget of NH_3 and its partitioning between gas and particle phase.

3.1. Ocean Model

We use two 3-D global ocean models: the biogeochemistry/ecosystem/circulation model (BEC), [*Moore et al.*, 2004], which is integrated in the Community Climate System Model 3 ocean circulation model, and the Carbon, Ocean Biogeochemistry and Lower Trophics model (COBALT), [*Stock et al.*, 2014a, 2014b], which is integrated in the Modular Ocean Model version 4p1 [*Griffies*, 2012]. These ecosystem models represent the transport and biogeochemical cycling of oceanic carbon, nitrogen, phosphate, silicate, and iron. BEC explicitly represents zooplankton, small phytoplankton, diatoms, and diazotrophs. COBALT includes a more detailed planktonic food web as well as bacteria. Organisms can meet their N requirements using both NH_x(sw) and NO_3^-(sw). NH_x(sw) is preferentially taken up over NO_3^- and NH_x(sw) concentration is generally less than 10% of the NO_3^-(sw) concentration [*Gruber*, 2008]. The uptake (v) of both NO_3^-(sw) and NH_x(sw) by small and large phytoplankton follows Michaelis-Menten kinetics when only one nitrogen form is present,

$$v_X = \frac{V_{max}[X]}{[X] + \kappa_X}$$

Table 2. Observations Used in This Study[a]

Mission	Time Frame	Reference
	Gas Phase NH_3	
AMT14	Apr–Jun 2004	*Johnson et al.* [2008]
AMT17	Oct–Nov 2005	*Johnson et al.* [2008]
ANT XXI/1	Oct–Nov 2006	*Keene et al.* [2009]
D267	Nov–Dec 2002	*Johnson et al.* [2008]
JR75	Jun–Jul 2002	*Johnson et al.* [2008]
R/V Oceanographer	Apr–May 1988	*Quinn et al.* [1990]
S18/01	Sep 1995	*Johnson et al.* [2008]
	Aerosol NH_4^+, Na^+, Cl^-, SO_4^{2-}[b]	
ACE1	Oct–Dec 1995	*Bates et al.* [1998]
ACE2	Jun–Jul 1997	*Raes et al.* [2000]
ACEASIA	Mar–Apr 2001	*Huebert et al.* [2003]
AEROINDO	Jan–Mar 1999	*Bates et al.* [2001]
AMT12	May–Jun 2003	*Baker et al.* [2010]
AMT13	Sep–Oct 2003	*Baker et al.* [2010]
AMT14	Apr–Jun 2004	*Baker et al.* [2010]
AMT15	Sep–Oct 2004	*Baker et al.* [2010]
AMT16[c]	May–Jun 2005	*Baker et al.* [2010]
AMT17	Oct–Nov 2005	*Baker et al.* [2010]
ANT XXI/1	Oct–Nov 2006	*Keene et al.* [2009]
ANT 23-1	Oct–Nov 2005	*Baker et al.* [2010]
DYNAMO	Oct–Dec 2011	*Yoneyama et al.* [2013]
FeeP	Apr–May 2004	*Dixon* [2008]
ICEALOT	Mar–Apr 2008	http://saga.pmel.noaa.gov/
INDOEX[c]	Feb–Mar 1998	*Krishnamurti et al.* [1998]
JCR	Sep–Oct 2001	*Baker et al.* [2010]
KH02-3	Sep–Oct 2002	*Nakamura et al.* [2005]
M55	Oct–Nov 2002	*Baker et al.* [2010]
PE203[c]	Oct 2002	*Sarthou et al.* [2007]
RITS93	Mar–May 1993	http://saga.pmel.noaa.gov/
RITS94	Nov 1993 to Jan 1994	http://saga.pmel.noaa.gov/
VOCALS	Oct–Nov 2008	*Wood et al.* [2011]
WACS2012	Aug 2012	http://saga.pmel.noaa.gov/
	Seawater NH_x	
AMT11	Oct–Nov 2000	http://amt-uk.org/
AMT12	May–Jun 2003	http://amt-uk.org/
AMT14	Apr–Jun 2004	*Johnson et al.* [2008]
AMT17	Oct–Nov 2005	*Johnson et al.* [2008]
ANTARES	Apr–May 1993	*Bianchi et al.* [1997]
Bermuda	Sep–Apr 1992	*Quinn et al.* [1996]
Bonus-GoodHope	Feb–Mar 2008	*Joubert et al.* [2011]
D253	May–Jun 2001	*Popova et al.* [2002]
D267	Nov–Dec 2002	*Johnson et al.* [2008]
EPREX	May–Jun 2000	*Sutka et al.* [2004]
JAMSTEC	Various	http://www.godac.jamstec.go.jp
JR75	Jun–Jul 2002	*Johnson et al.* [2008]
PS211	Sep 1995	*Johnson et al.* [2008]

Table 2. (continued)

Mission	Time Frame	Reference
RITS94	Nov 1993 to Jan 1994	http://saga.pmel.noaa.gov/
KN182-09	October 2005	*Fernández et al.* [2009]
R/V Oceanographer	Apr – May 1988	*Quinn et al.* [1990]
R/V Meteor	Mar – Apr 2003	*Kuypers et al.* [2005]
S18/01	Dec 2001	*Johnson et al.* [2008]
	U.S. Joint Global Ocean Flux Study	
– NABE	Apr – July 1989	*Ducklow and Harris* [1993]
– EqPac	Jan – Dec 1992	*Murray et al.* [1995]
– Arabian Sea	Jan – Dec 1995	*Smith et al.* [1998]
– AESOPS	Aug 1996 to Mar 1998	*Smith et al.* [2000]

[a]The location of the different cruises is given in Figure S1.
[b]Fine mode except otherwise noted.
[c]Fine + coarse.

where X can be either $NH_x(sw)$ or $NO_3^-(sw)$ and V_{max} is the maximum uptake rate. In COBALT $NO_3^-(sw)$ uptake is reduced in inverse proportion to the degree of $NH_x(sw)$ saturation [*Frost and Franzen*, 1992], reflecting the redox favorability of $NH_x(sw)$ for phytoplankton growth. For both $NO_3^-(sw)$ and $NH_x(sw)$, v_X is controlled by the half saturation (κ_X). The stronger affinity of phytoplankton for $NH_x(sw)$ is reflected by a lower half saturation for $NH_x(sw)$ than for $NO_3^-(sw)$ (Table 3). COBALT and BEC use very different half saturations for $NH_x(sw)$ but the same half saturations for $NO_3^-(sw)$. This reflects the large range of measured ammonium half saturations: 0.1 – 0.5 mmol m^{-3} [*Eppley et al.*, 1969], 0.02 – 0.6 mmol m^{-3} [*Shiomoto et al.*, 1994], and 0.01 – 0.08 mmol m^{-3} [*Harrison et al.*, 1996]. Both BEC and COBALT include nitrification as an additional sink for $NH_x(sw)$ and account for its postulated inhibition by light [*Ward et al.*, 1982; *Yool et al.*, 2007; *Smith et al.*, 2014]. Neither model includes anammox [*Gruber*, 2008]. NH_x sources are dominated by the biological remineralization of organic matter (~7 PgN a^{-1} and 6 PgN a^{-1} in the upper 100 m in COBALT and BEC, respectively). External sources of N to the ocean include atmospheric deposition and riverine nitrogen based on Global-NEWS (for COBALT only from *Seitzinger et al.* [2005]) and are much smaller (~130 $TgNa^{-1}$ [*Gruber*, 2004]) than biological remineralization.

For COBALT, we use a monthly climatology of surface $NH_x(sw)$ and $H^+(sw)$ derived from the last 20 years of a 1060 year preindustrial control run of the Earth System Model ESM2M from the Geophysical Fluid Dynamics Laboratory (GFDL), [*Dunne et al.*, 2012, 2013; *Stock et al.*, 2014b]. For BEC, we use results from a historical simulation of the CCSM3 ocean model for the late 20th century and early 21st century [*Doney et al.*, 2009]. The CCSM3 baseline simulation was spun up for approximately 800 years using a repeat annual cycle of physical forcing and dust deposition. A 54 year hindcast was then conducted using National Centers for Environmental Prediction atmospheric reanalysis, satellite, and climatological surface forcing beginning in year 1959. Here we use a 12 month climatology computed from the last 10 years of the simulation for both $NH_x(sw)$ and $H^+(sw)$.

Table 3. Half Saturation κ_X (Equation (1)) for Plankton Uptake of $NO_3^-(sw)$ and $NH_4^+(sw)$[a]

	Small Phytoplankton			Large Phytoplankton		
	BEC	COBALT	COBALT-HA	BEC	COBALT	COBALT-HA
NH_4^+	0.005	0.1	0.02	0.08	0.5	0.1
NO_3^-	0.5	0.5	0.5	2.5	2.5	2.5

[a]Value in mmol m^{-3} for the BEC model [*Moore et al.*, 2004], the COBALT model [*Stock et al.*, 2014a], and the high-affinity COBALT model (COBALT-HA) implemented in this paper by reducing κ by a factor of 5 from the standard COBALT model.

3.2. Atmosphere-Ocean Exchange of NH_3

We follow *Liss and Slater* [1974] to represent the bidirectional exchange of NH_3 between ocean and atmosphere. The net flux F of NH_3 from the ocean to the atmosphere is calculated as

$$F = -K\left([NH_3] - H^{\star}[NH_x(sw)]\right) \tag{1}$$

where $[NH_3]$ and $[NH_x(sw)]$ are the gas and seawater concentrations of ammonia and NH_x, respectively, $H^{\star}$ is the dimensionless effective gas-over-liquid Henry's law constant for NH_x and K is the transfer velocity between atmosphere and ocean

$$H^{\star} = \frac{H}{1 + 10^{-p\mathrm{H}+p\mathrm{Ka}}} \tag{2}$$

$$K = \left[\frac{1}{k_g} + \frac{H^{\star}}{k_w}\right]^{-1} \tag{3}$$

where H is the actual dimensionless Henry's law constant for NH_3, pKa is the $-\log_{10}$ of the acid dissociation constant for NH_4^+/NH_3, and k_g and k_w are the transfer velocities in the gas phase and water, respectively. We use the pH simulated by BEC and COBALT in the surface layer (12 m and 10 m deep, respectively). H and pKa are calculated following *Johnson et al.* [2008] and *Bell et al.* [2007]:

$$H = \left(\frac{17.93T}{273.15}\exp\left(\frac{4092}{T} - 9.7\right)\right)^{-1} \tag{4}$$

$$p\mathrm{Ka} = 10.04 - 3.16 \times 10^{-2}(T - 273.15) + 3.1 \times 10^{-3}S \tag{5}$$

where T is the temperature (K) and S the salinity (practical salinity unit). $k_g(m\,s^{-1})$ is calculated following *Johnson* [2010]:

$$k_g = 10^{-3} + \frac{u_{\star}}{13.3Sc_a + C_D^{-\frac{1}{2}} - 5 + \frac{\ln(Sc_a)}{2\kappa}} \tag{6}$$

where $u_{\star}$ is the friction velocity (m s^{-1}), Sc_a is the airside Schmidt number, C_D is the drag coefficient, and κ is the von Karman constant ($\kappa = 0.4$). Following *Smith* [1980], we estimate C_D and $u_{\star}$ from the 10 m wind velocity (u_{10} in m s^{-1}) as $C_D = (u_{\star}/u_{10})^2 = 6.1 \times 10^{-4} + 6.3 \times 10^{-5}u_{10}$ and $u_{\star} = u_{10}\sqrt{6.1 \times 10^{-4} + 6.3 \times 10^{-5}u_{10}}$. k_w (cm h^{-1}) is calculated following *Nightingale et al.* [2000]:

$$k_w = \left(0.24u_{10}^2 + 0.061u_{10}\right)\sqrt{\frac{Sc_{600}}{Sc_{NH_3}}} \tag{7}$$

where Sc_{600} is the Schmidt number for CO_2 in freshwater at 20° C ($Sc_{600} = 600$) and Sc_{NH_3} is the Schmidt number for NH_3 in water [*Johnson*, 2010]. Under ambient conditions (temperature, salinity, pH), $K \simeq k_g$ for NH_3 [*Beale et al.*, 2014].

3.3. Atmospheric Model

We use the GEOS-Chem global 3-D chemical transport model v9.01–03 (www.geos-chem.org) to simulate the fate of NH_x in the atmosphere. All simulations are performed for 2006 and are preceded by a 6 month-long spin-up. The model is driven by assimilated meteorological data from the NASA Goddard Earth Observing System (GEOS-5) with horizontal resolution of 0.5° × 0.67°and 72 vertical levels. We degrade the horizontal resolution to 2° × 2.5°for use in GEOS-Chem.

In the atmosphere, NH_x can exist in the gas phase as NH_3 and in the particle phase as NH_4^+. Marine observations show that NH_4^+ is primarily found in the fine mode (diameter <2.5 μ*m*), and we neglect coarse mode NH_4^+ [*Fridlind and Jacobson*, 2000; *Baker et al.*, 2010]. We use ISORROPIA [*Fountoukis and Nenes*, 2007] to simulate the thermodynamic equilibrium between non-sea-salt sulfate ($nss - SO_{4T} \equiv SO_4^{2-} + HSO_4^- + H_2SO_4$), $NO_{3T} \equiv HNO_3 + NO_3^-$, $Cl_T = HCl + Cl^-$, $NH_x \equiv NH_3 + NH_4^+$, and Na^+.

The presence of nss-SO_{4T} shifts the partitioning of ammonia from gas to the favored particle phase over the gas phase. Far from coastal regions, the principal source of nss-SO_{4T} is DMS oxidation [*Chin and Jacob*, 1996].

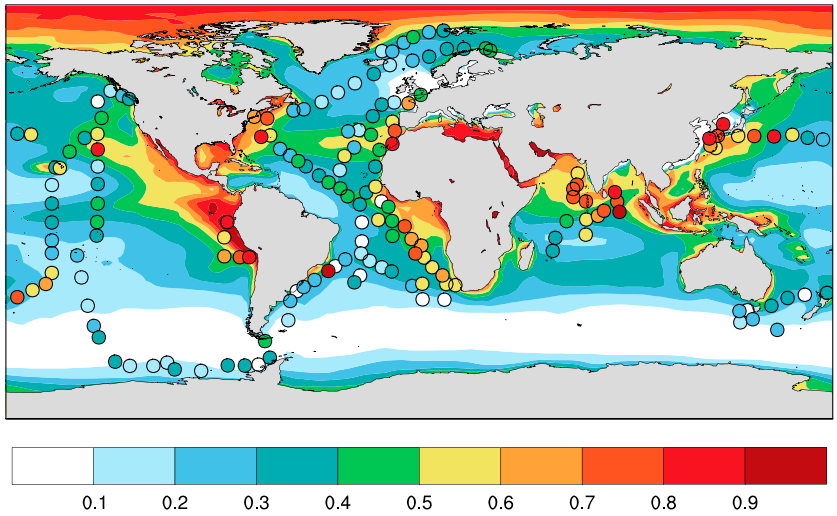

Figure 1. Chloride depletion in fine sea salt aerosol in surface air. The figure shows the deficit in the aerosol Cl^-:Na^+ ratio relative to sea salt composition (0 means no depletion, 1 means total depletion). Annual mean values from GEOS-Chem (background) are compared to the ship measurements (circles). The measurements are averaged onto a 7.5° × 7.5°grid for readability.

Marine emissions of DMS are calculated using the monthly climatology of seawater DMS from *Lana et al.* [2011] and k_w (from equation (7)). The resulting annual flux is 22.5 TgS a^{-1}, which falls within the range of emissions calculated by *Lana et al.* [2011] (17.6–34.4 $TgSa^{-1}$) and is 20% lower than their central estimate (28.1 TgS a^{-1}).

The partitioning of NH_x between gas and particle phases is also affected by the degree of mixing between fine sea salt and nss-SO_{4T}. In the standard GEOS-Chem model, Cl_T (≡ HCl + Cl^-) and Na^+ are not treated explicitly but calculated based on the atmospheric concentration of fine mode sea salt [*Jaeglé et al.*, 2011] and the average abundance of Na^+ and Cl^- in seawater. In the accumulation mode, sea salt and nss-SO_{4T} are assumed to be completely mixed. This treatment favors gas phase NH_3 and HCl since sea salt alkalinity neutralizes some of the sulfate acidity (which would otherwise be neutralized by NH_3 uptake) and HCl is volatilized in the process [*Fridlind and Jacobson*, 2000]. Similar assumptions are made in other global chemical transport models [*Feng and Penner*, 2007; *Luo et al.*, 2007]. Here we prescribe the fraction $f_{NaCl}^{SO_4}$ of nss-SO_4 that is internally mixed with fine sea salt and explicitly account for the volatilization of HCl. We find that with $f_{NaCl}^{SO_4} = 0.5$, GEOS-Chem can capture the magnitude and spatial distribution of chloride depletion (i.e., $1 - ([Cl^-]/[Na^+])/([Cl^-(sw)]/[Na^+(sw)])$) well away from coastal regions (Figure 1).

Global anthropogenic sources of NH_3 are taken from the Global Emissions InitiAtive (GEIA), which is based on the work of *Bouwman et al.* [1997]. For biofuel and other nonagricultural sources, we use emissions from the Atmospheric Chemistry and Climate Model Intercomparison Project [*Lamarque et al.*, 2010]. In the U.S., Canada, Europe, and East Asia, anthropogenic NH_3 emissions are based on the National Emission Inventory from the U.S. EPA (http://www.epa.gov/ttnchie1/net/2005inventory.html), the Criteria Air Contaminant inventory (http://www.ec.gc.ca/air/default.asp?lang=En&n=7C43740B-1), the European Monitoring and Evaluation Programme [*Centre on Emission Inventories and Projections*, 2013], and *Streets et al.* [2003] inventories, respectively. Open fire emissions are taken from the Global Fire Emissions Database version 3 with monthly resolution [*van der Werf et al.*, 2010]. Soil and wildlife emissions are taken from GEIA [*Bouwman et al.*, 1997]. Here we also include NH_3 emissions from volcanoes (0.9 TgN a^{-1}) and sea bird colonies (0.22 TgN a^{-1} [*Riddick et al.*, 2012]). Following *Sutton et al.* [2008], volcanic emissions are calculated using a molar ratio of NH_3 to SO_2 of 0.15 as reported by *Uematsu et al.* [2004]. Our estimate of the magnitude of volcanic sources is twice as large as that of *Sutton et al.* [2008] reflecting larger volcanic SO_2 emissions (13 $TgSa^{-1}$ [*Fisher et al.*, 2011]). Table 1 summarizes our inventory of natural NH_3 emissions. Terrestrial natural emissions are 7.1 TgN a^{-1}, as compared to 38 TgN a^{-1} for anthropogenic emissions (mainly from agriculture).

The representation of wet deposition in GEOS-Chem accounts for scavenging in convective updrafts as well as in-cloud and below-cloud scavenging from large-scale precipitation. Aerosol NH_4^+ is fully incorporated in cloud droplets and ice crystals [*Liu et al.*, 2001; *Wang et al.*, 2011]. NH_3 is scavenged by warm clouds and rain

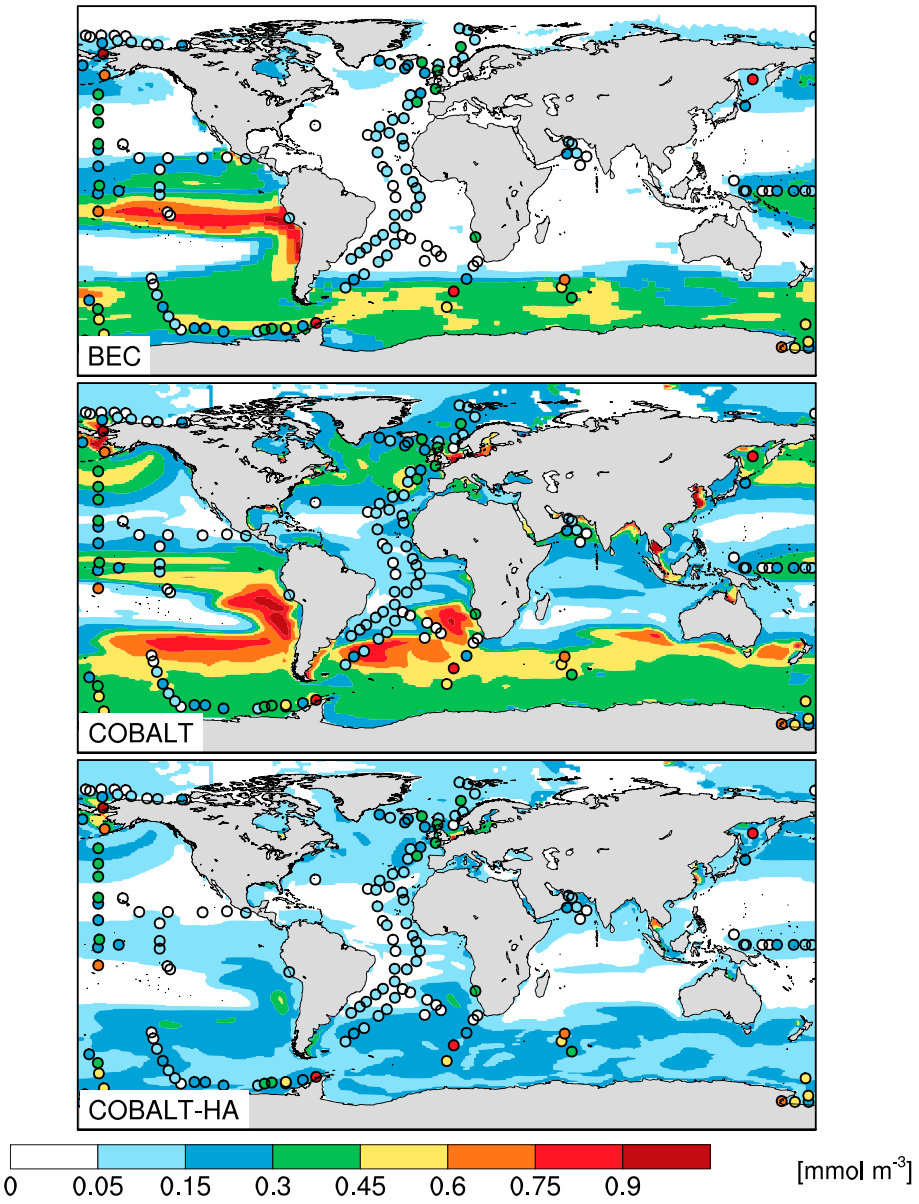

Figure 2. Surface seawater concentration (depth < 20 m) of total ammonia(NH_x(sw)). Annual mean values from the (top) BEC, (middle) COBALT, and (bottom) COBALT-HA models (background) are compared to the ship measurements (circles). The measurements are averaged onto a 7.5° × 7.5° grid for readability.

on the basis of its solubility in water [*Amos et al.*, 2012] with a retention coefficient of 5% for riming in mixed clouds [*Wang et al.*, 2008]. NH_3 is not scavenged by cold (ice) clouds. *Fisher et al.* [2011] found little sensitivity of the GEOS-Chem simulation of NH_4^+ to the assumptions made for $NH_3(g)$ scavenging in mixed and cold clouds.

4. Results and Discussion

4.1. Comparison With Seawater Observations

Figure 2 shows the observed concentrations of NH_x(sw) in surface water and the simulated annual distributions in BEC and COBALT. Observations show a maximum in the Southern Ocean and a minimum in subtropical gyres where concentrations are often below detection limit. The median observed [NH_x(sw)] is 0.07 mmol m^{-3} with 50% of the observations between 0.02 and 0.22 mmol m^{-3}.

COBALT generally predicts greater concentrations of NH_x(sw) than BEC due to the use of a greater half saturation constant for NH_x(sw) (Table 3). Consistent with observations, both BEC and COBALT show greater

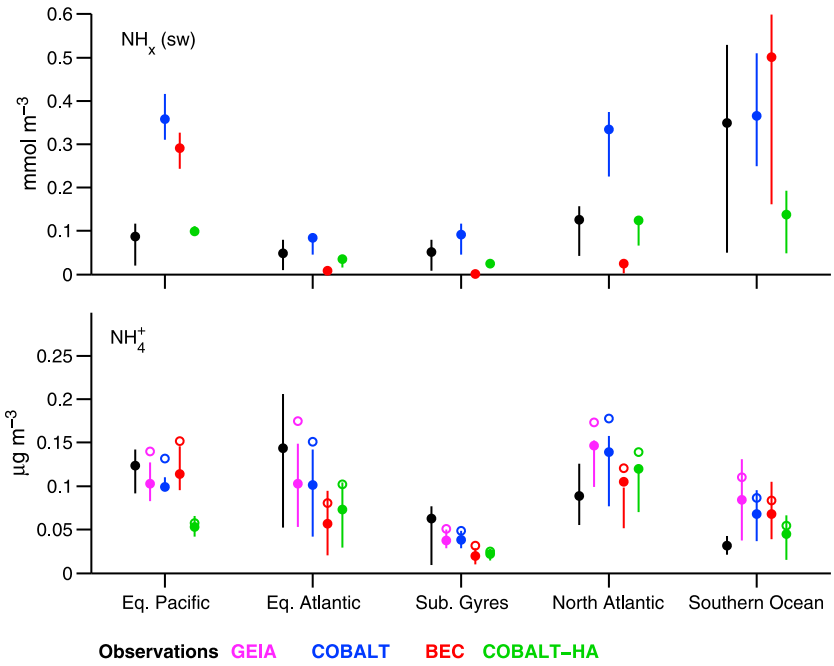

Figure 3. Mean concentration of total surface (top) seawater ammonia NH_x(sw) and (bottom) aerosol ammonium NH_4^+ in different oceanic regions. Equatorial Pacific and Atlantic regions are defined as the high-chlorophyll regions (annual average chlorophyll > 0.15 mg m^{-3}) within 30°of the equator. The subtropical gyres are defined as low-chlorophyll regions (annual average chlorophyll < 0.05 mg m^{-3}) within 40°of the equator. The North Atlantic is defined as north of 40°N and the Southern Ocean is defined as south of 40°S. We exclude NH_4^+ observations with modeled or observed nss-SO_{4T} exceeding 1 $\mu g\, m^{-3}$ to limit continental influence. The bars indicate the 25th and 75th percentiles. The open circles in Figure 3 (bottom) show the simulated atmospheric NH_x. COBALT (blue), BEC (red), and COBALT-HA (green) refer to the different ocean biogeochemical models, whose simulated distributions of [NH_x(sw)] are used to calculate ocean NH_3 emissions in GEOS-Chem. Simulated [NH_4^+] concentrations based on the GEIA ocean emissions are also shown (purple). The simulated distribution of [NH_x(sw)] and [NH_4^+] are sampled to match the month and location of the observations.

concentrations of NH_x(sw) in the Equatorial Pacific and Southern Ocean than in the subtropical gyres. In both models, the elevated concentration of NH_x(sw) in the Equatorial Pacific and Southern Ocean is associated with iron limitation of phytoplankton growth. In contrast, phytoplankton growth is predominately nitrogen limited in the Atlantic Ocean which leads to very low concentrations of NH_x(sw). The greater contrast between the Equatorial Atlantic and the Equatorial Pacific for [NH_x(sw)] in BEC relative to COBALT may reflect different treatments of the modulation of nitrate uptake by NH_x(sw) and of multiple nutrient limitations on growth. COBALT overestimates observed [NH_x(sw)] in the Southern Pacific and Atlantic consistent with *Stock et al.* [2014a], who showed that nutrient-rich waters associated with the Southern Ocean extend too far north in COBALT.

Figure 3 (top) shows mean observed and simulated NH_x(sw) concentrations in different oceanic regions. BEC is biased high in the nutrient-rich Equatorial Pacific and Southern Ocean by over a factor of 3. In the nutrient-poor subtropical gyres and in the Equatorial Atlantic, BEC underestimates [NH_x(sw)] by over a factor of 3. In contrast, COBALT is biased high by a factor of 2 in both nutrient-rich and nutrient-poor regions.

The heterogeneity of the biases and the very low concentrations of NH_x(sw) in the Atlantic basin in BEC (Figure 2) are indicative of uncertainties in the treatment of nutrient limitation and thus cannot be easily reduced through a single parameter. In contrast, the spatial homogeneity of the high bias in COBALT suggests that a simple calibration of ammonia half saturation may improve the simulations of [NH_x(sw)]. The rationale for this strategy is bolstered by the large uncertainty in the half-saturation constants for ammonia uptake, and the fact that COBALT uses a half saturation near the high end of the observations. We thus conducted a simulation with a "high-affinity" version of COBALT (referred to as COBALT-HA hereafter) where the ammonia half-saturation constants for all phytoplankton groups were decreased by a factor of 5 (Table 3). These values remain within the observed range, in particular, the results of *Shiomoto et al.* [1994] and *Harrison et al.* [1996]

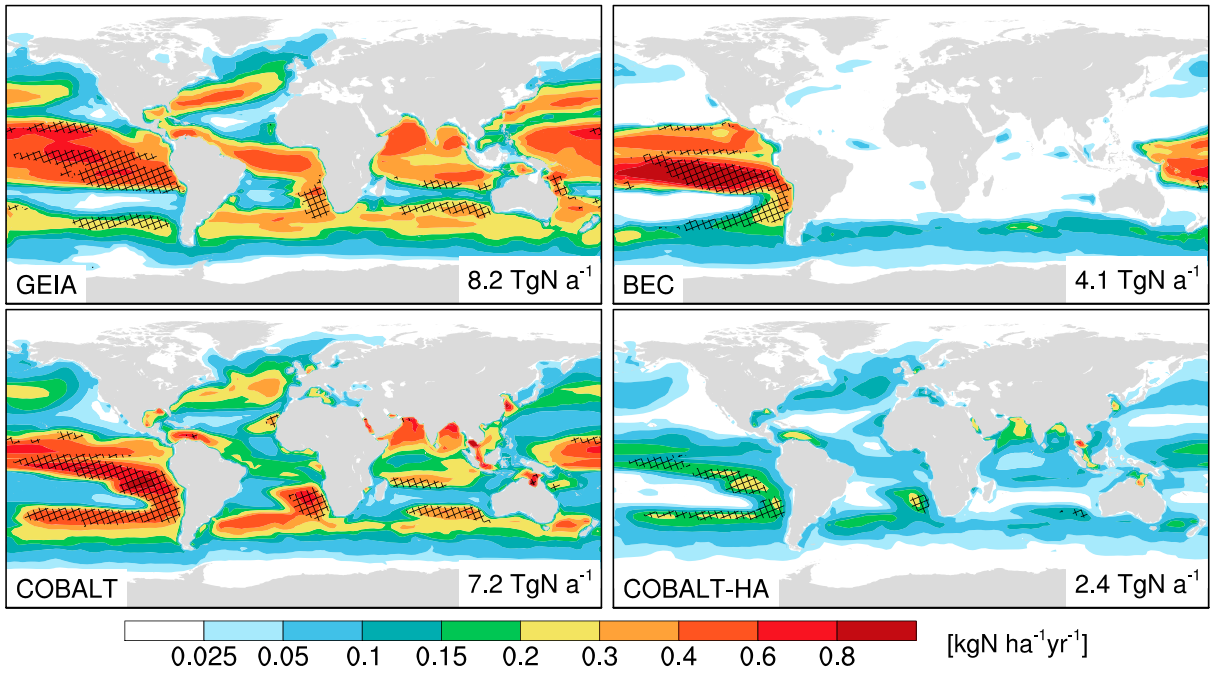

Figure 4. Annual gross oceanic emissions of NH_3 calculated using simulated [NH_x(sw)] from the BEC, COBALT, and COBALT-HA ocean biogeochemical models (see equation (1)). Ocean emissions from the GEIA inventory are also shown. Total ocean gross emissions of NH_3 are indicated inset. Hatches denote regions where the ocean is a net source of reduced nitrogen to the atmosphere, i.e., where the net flux of NH_3 from the ocean (equation (1)) exceeds the total deposition of NH_4^+.

and higher than the values used in BEC. Figure 2 (bottom) shows that the simulated response of NH_x(sw) concentration to a change in κ_X is fairly homogeneous with a 3–4-fold decrease of surface [NH_x(sw)]. Other ecosystem properties (e.g., chlorophyll, [NO_3^-(sw)]) remain relatively constant since they are dictated by the community response to the large-scale supply of nutrients and light that remain unchanged (Figures S2 and S3 in the supporting information). COBALT-HA compares more favorably with the observations than either BEC or COBALT. Basin-averaged [NH_x(sw)] falls within the interquartile range of observed [NH_x(sw)] in all regions shown in Figure 3 (top).

4.2. Emissions

Figure 4 shows the spatial distribution of the gross ocean to air flux of NH_3 (i.e., K H*[NH_x(sw)] in equation (1)) calculated using [NH_x(sw)] from COBALT, BEC, and COBALT-HA as well as the estimate from *Bouwman et al.* [1997] (referred to as GEIA hereafter). We focus on the gross flux as it is independent of the atmospheric fate of NH_x and allows for direct comparison with previous estimates of ocean emissions (Table 1).

The simulated gross ocean source of NH_3 ranges from 2 to 8 TgN a^{-1}. In all models, simulated emissions are maximum in the Equatorial Pacific and minimum at high latitudes. This meridional gradient is driven more by the dependence of NH_3 solubility on temperature (equations (4) and (5)) rather than by the distribution of NH_x(sw) in agreement with field data [*Johnson et al.*, 2008]. Emissions driven by COBALT-HA, which are most consistent with [NH_x(sw)] observations (Figures 2 and 3, top), yield the lowest gross flux, almost 4 times lower than that estimated by *Bouwman et al.* [1997]. Figure 4 also shows regions where the ocean is a net source of reduced nitrogen to the atmosphere. All models show that the Equatorial and Southern Pacific are net sources of reduced nitrogen, while the North Atlantic is a net sink. In the simulations driven by COBALT and GEIA, parts of the North Pacific and Indian oceans are also net sources of reduced nitrogen.

Figure 5 (top left) shows that the low oceanic emissions inferred from COBALT-HA imply that continental influences on atmospheric NH_x in surface air extend over most of the ocean. The Equatorial Pacific and portions of the Southern Ocean are the only regions where ocean emissions contribute over 70% of NH_x in surface air. In the North Atlantic and Pacific, ocean emissions generally contribute less than 50% of NH_x. Over the Southern Ocean, the influence of anthropogenic emissions is small but aviary emissions (0.18 TgN a^{-1} in the Southern Ocean) have a large regional influence, consistent with island and coastal observations

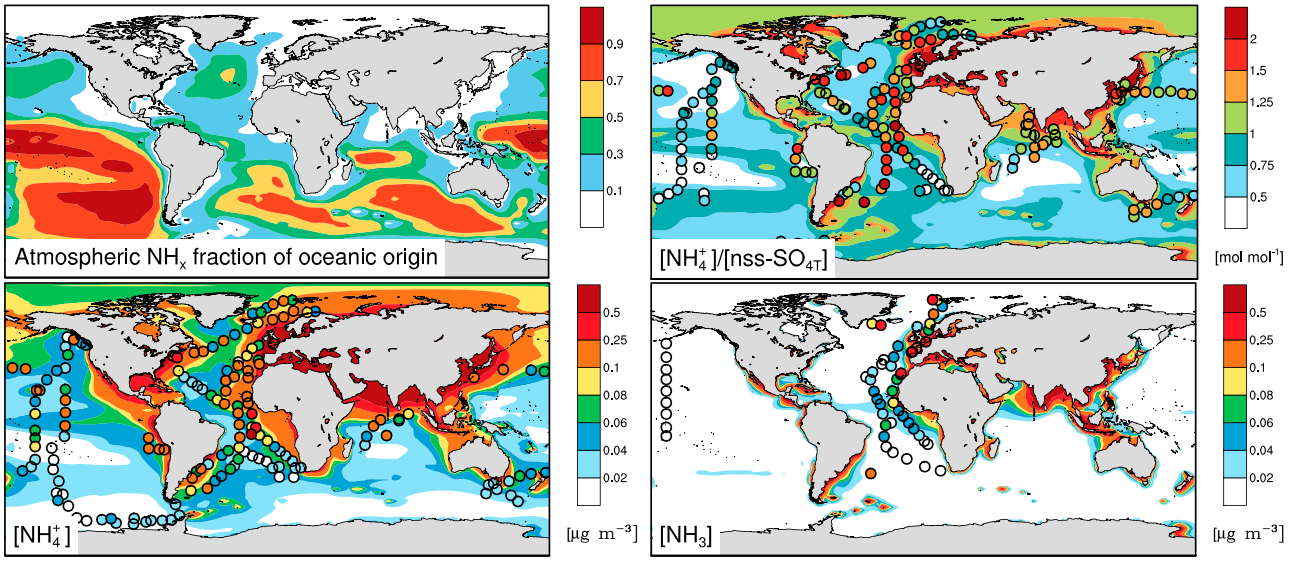

Figure 5. Atmospheric distribution of total ammonia (NH_x) in surface air over the ocean. Annual mean values from the GEOS-Chem simulation driven by COBALT-HA seawater [NH_x(sw)] (background) are compared to ship measurements (circles). (top left) The model contribution of ocean emissions to [NH_x]. (top right) The fractional neutralization of non-sea-salt sulfate by ammonia as expressed by the molar ratio of NH_x to non-sea-salt total sulfate (nss-SO_{4T}). (bottom left) The concentrations of aerosol NH_4^+ and (bottom right) gas phase NH_3. The observations are averaged onto a 7.5° × 7.5°grid for readability. For NH_4^+, we exclude observed values with nss SO_{4T} exceeding 1 μg m^{-3} to limit the influence of continental sources.

[*Legrand et al.*, 1998, 2012]. The large influence of nonmarine sources over most of the ocean limits our ability to test the model representation of the marine source. Thus, we will focus our model evaluation on the Equatorial Pacific and Southern Ocean where the marine source makes a major contribution.

4.3. Comparison With Atmospheric Observations

Figure 5 (top right panel) shows that when GEOS-Chem is driven by COBALT-HA the simulated molar ratio of NH_x to nss − SO_{4T} concentrations is generally less than 2 over much of the remote ocean, consistent with observations [see also *Phinney et al.*, 2006; *Zorn et al.*, 2008]. Under these conditions, aerosols are highly acidic and most NH_x is in the particulate phase, such that NH_4^+ is sensitive to ocean NH_3 emissions. Figure 5 also shows simulated and observed NH_4^+ concentrations (bottom left panel). Away from continental influence, observations show a maximum in the Equatorial Pacific and a minimum in the subtropics and Southern Ocean. This spatial distribution is broadly captured by GEOS-Chem driven by COBALT-HA [NH_x(sw)].

Figure 3 compares simulated and observed NH_4^+ concentrations in the same regions used for evaluating simulated [NH_x(sw)]. We also include simulated NH_x concentrations (open circles). In the simulations driven by COBALT, BEC, or GEIA, NH_3 can represent a large fraction of NH_x, such that uncertainties in the partitioning of NH_x between gas and particle phases (e.g., from nss − SO_4^{2-} and the degree to which it is internally mixed with sea salt) may obscure the relationship between [NH_4^+] and ocean NH_3 emissions. However, in COBALT-HA, NH_4^+ comprises most of NH_x and simulated [NH_4^+] is more directly related to ocean NH_3 emissions.

We first focus on the Southern Ocean and Equatorial Pacific where simulated [NH_4^+] is least impacted by nonoceanic NH_3 emissions. In the Southern Ocean, GEOS-Chem driven by COBALT-HA shows improved performance compared to other model configurations (40% high bias). However, COBALT-HA [NH_4^+] is biased low in the Equatorial Pacific by over 50% even though it provides a good simulation of [NH_x(sw)] in this region. COBALT-HA is also biased low over the Equatorial Atlantic (−50%) and subtropical gyres (-65%). Overall GEOS-Chem underestimates [NH_4^+] by 35% when driven by COBALT-HA [NH_x(sw)]. GEOS-Chem predicts that [NH_x] is significantly impacted by nonoceanic sources of NH_3 over many regions sampled by the research cruises used in this study. The underestimate of [NH_x] may thus be partly driven by uncertainties in the magnitude of continental sources of NH_3 and in the long-range transport of NH_x. Isotopic measurements of [NH_4^+] in precipitation [*Altieri et al.*, 2014] may provide better constraints on the contribution of continental sources to marine atmospheric NH_x.

In the Equatorial Pacific the influence of nonoceanic sources is predicted to be small, which suggests that additional marine sources of NH_3 may exist. A possible source is the photolysis of dissolved organic nitrogen (DON) either in seawater or in the atmosphere. In the atmosphere, NH_3 may be produced by the photooxidation of amines [*Nielsen et al.*, 2011], which are important contributors to marine secondary organic aerosols [*Facchini et al.*, 2008]. *Zhang and Anastasio* [2003] also reported production of NH_4^+ from the photolysis of aerosol organic nitrogen, which may involve deamination of amino acids [*Milne and Zika*, 1993]. In seawater, the production of $NH_x(sw)$ from the photolysis of DON has been demonstrated in many regions of the ocean [*Bushaw et al.*, 1996; *Morell and Corredor*, 2001; *Kitidis et al.*, 2006; *Aarnos et al.*, 2012; *Xie et al.*, 2012; *Rain-Franco et al.*, 2014]. The vertical resolution of the [$NH_x(sw)$] observations used here (~10m) is not sufficient to evaluate any enhancement in [$NH_x(sw)$] near the surface. Reproducing the observations of aerosol [NH_4^+] in the Equatorial Pacific would require a doubling of the ocean NH_3 source in this region. Assuming a similar underestimate in other regions suggests that ocean emissions of NH_3 are in the range 2–5 TgN a^{-1}. More combined observations of $NH_x(sw)$, NH_3, and NH_4^+ [e.g., *Norman and Leck*, 2005] in different seasons are needed to further our understanding of the budget of atmospheric reduced nitrogen in the marine atmosphere.

5. Conclusion

Current global inventories of NH_3 emissions identify the ocean as the dominant natural source and the most important overall source of NH_3 in many remote oceanic regions. We examined the constraint on that source using a large ensemble of ship NH_3/NH_4^+ observations in the surface ocean and in marine air. Evaluation of two global ocean biogeochemistry models (COBALT and BEC) indicates that they overestimate the concentrations of total seawater ammonia concentrations ($NH_x(sw)$). Better results are achieved in the COBALT model by assuming higher affinity of plankton for ammonia. The resulting model (COBALT-HA) implies a much smaller gross ocean source of ammonia to the atmosphere (2.5 TgN a^{-1}). This estimate is much lower than the GEIA emission inventory (8 TgN a^{-1}) that is widely used in global atmospheric composition models.

We examined the implication of this lower ocean emission to the atmosphere in terms of atmospheric concentrations of NH_3 and NH_4^+ over the ocean simulated by the GEOS-Chem global chemical transport model. We find that long-range transport from continental sources is the dominant source of NH_x over most oceanic regions. The ocean source dominates only over the Equatorial Pacific and parts of the Southern Ocean. Simulated marine aerosols are highly acidic over most of the ocean, consistent with observations. The GEOS-Chem model driven by COBALT-HA provides, in general, a good simulation of observed aerosol NH_4^+ concentrations over the ocean. An exception is the Equatorial Atlantic and Pacific where simulated [NH_4^+] is biased low by over twofold. This discrepancy suggests that other processes may contribute to the release of NH_3 from the ocean. We speculate that an additional source of NH_3 may originate from the photolysis of dissolved organic nitrogen in the surface water or in the atmosphere. Accommodating this missing source, we conclude that the gross oceanic source of ammonia to the atmosphere is in the range of 2–5 TgN a^{-1}, significantly lower than current estimates. This implies that the ocean source is comparable to terrestrial natural sources from open fires and from soils and that the anthropogenic perturbation to atmospheric reduced nitrogen may be even greater than previously estimated [*Galloway et al.*, 2004].

Acknowledgments
This work was funded by NASA ACMAP. S. C. Doney, I. D. Lima, and W. C. Keene acknowledge support from NSF (AGS-1020594 and EF-0424599 to WHOI and AGS-0328342 to UVA). T. G. Bell acknowledges support from the UK SOLAS Knowledge Transfer grant (SOLAS Project Integration; NE/E001696/1). We thank T. Suzuki, P. Quinn, and A. Pszenny for contributing observations of marine nitrogen, B. Ward for helpful discussions, and L. W. Horowitz, J. P. Dunne, and two anonymous reviewers for their comments on the manuscript. Model outputs presented in this study are available upon request (Fabien.Paulot@noaa.gov).

References

Aarnos, H., P. Ylöstalo, and A. V. Vähätalo (2012), Seasonal phototransformation of dissolved organic matter to ammonium, dissolved inorganic carbon, and labile substrates supporting bacterial biomass across the Baltic Sea, *J. Geophys. Res.*, *117*, G01004, doi:10.1029/2010JG001633.

Aiken, J., and A. J. Bale (2000), An introduction to the Atlantic Meridional Transect (AMT) programme, *Prog. Oceanogr.*, *45*(3–4), 251–256, doi:10.1016/S0079-6611(00)00004-5.

Almeida, J., et al. (2013), Molecular understanding of sulphuric acid-amine particle nucleation in the atmosphere, *Nature*, *7471*, 359–363, doi:10.1038/nature12663.

Altieri, K. E., M. G. Hastings, A. J. Peters, S. Oleynik, and D. M. Sigman (2014), Isotopic evidence for a marine ammonium source in rainwater at Bermuda, *Global Biogeochem. Cycles*, *28*, 1066–1080, doi:10.1002/2014GB004809.

Amos, H. M., et al. (2012), Gas-particle partitioning of atmospheric Hg(II) and its effect on global mercury deposition, *Atmos. Chem. Phys.*, *12*(1), 591–603.

Baker, A. R., T. Lesworth, C. Adams, T. D. Jickells, and L. Ganzeveld (2010), Estimation of atmospheric nutrient inputs to the Atlantic Ocean from 50°N to 50°S based on large-scale field sampling: Fixed nitrogen and dry deposition of phosphorus, *Global Biogeochem. Cycles*, *24*, GB3006, doi:10.1029/2009GB003634.

Ball, S. M., D. R. Hanson, F. L. Eisele, and P. H. McMurry (1999), Laboratory studies of particle nucleation: Initial results for H_2O, and NH_3 vapors, *J. Geophys. Res.*, *104*(D19), 23,709–23,718, doi:10.1029/1999JD900411.

Bates, T. S., B. J. Huebert, J. L. Gras, F. B. Griffiths, and P. A. Durkee (1998), International global atmospheric chemistry (IGAC) project's first aerosol characterization experiment (ACE 1): Overview, *J. Geophys. Res.*, *103*(D13), 16,297–16,318, doi:10.1029/97JD03741.

Bates, T. S., P. K. Quinn, D. J. Coffman, J. E. Johnson, T. L. Miller, D. S. Covert, A. Wiedensohler, S. Leinert, A. Nowak, and C. Neusüss (2001), Regional physical and chemical properties of the marine boundary layer aerosol across the Atlantic during Aerosols99: An overview, *J. Geophys. Res.*, *106*(D18), 20,767–20,782, doi:10.1029/2000JD900578.

Beale, R., M. T. Johnson, P. S. Liss, and P. D. Nightingale (2014), 8.3 - Air-sea exchange of marine trace gases, in *Treatise on Geochemistry (Second Edition)*, edited by H. D. H. K. Turekian, pp. 53–92, Elsevier, Oxford, U. K.

Bell, T. G., M. T. Johnson, T. D. Jickells, and P. S. Liss (2007), Ammonia/ammonium dissociation coefficient in seawater: A significant numerical correction, *Environ. Chem.*, *4*(3), 183–186.

Benson, D. R., J. H. Yu, A. Markovich, and S.-H. Lee (2011), Ternary homogeneous nucleation of H_2SO_4, NH_3, and H_2O under conditions relevant to the lower troposphere, *Atmos. Chem. Phys.*, *11*(10), 4755–4766, doi:10.5194/acp-11-4755-2011.

Berndt, T., et al. (2010), Laboratory study on new particle formation from the reaction OH + SO_2: Influence of experimental conditions, H_2O vapour, NH_3 and the amine tert-butylamine on the overall process, *Atmos. Chem. Phys.*, *10*(15), 7101–7116, doi:10.5194/acp-10-7101-2010.

Bianchi, M., F. Feliatra, P. Tréguer, M.-A. Vincendeau, and J. Morvan (1997), Nitrification rates, ammonium and nitrate distribution in upper layers of the water column and in sediments of the Indian sector of the Southern Ocean, *Deep Sea Res., Part II*, *44*(5), 1017–1032.

Bouwman, A. F., D. S. Lee, W. A. H. Asman, F. J. Dentener, K. W. Van Der Hoek, and J. G. J. Olivier (1997), A global high-resolution emission inventory for ammonia, *Global Biogeochem. Cycles*, *11*(4), 561–587.

Bushaw, K. L., R. G. Zepp, M. A. Tarr, D. Schulz-Jander, R. A. Bourbonniere, R. E. Hodson, W. L. Miller, D. A. Bronk, and M. A. Moran (1996), Photochemical release of biologically available nitrogen from aquatic dissolved organic matter, *Nature*, *381*(6581), 404–407.

Centre on Emission Inventories and Projections (2013), EMEP emissions, Austrian Environment Agency. [Available at http://www.ceip.at/.]

Chin, M., and D. J. Jacob (1996), Anthropogenic and natural contributions to tropospheric sulfate: A global model analysis, *J. Geophys. Res.*, *101*(D13), 18,691–18,699, doi:10.1029/96JD01222.

Clarke, A. D., and J. N. Porter (1993), Pacific marine aerosol: 2. Equatorial gradients in chlorophyll, ammonium, and excess sulfate during SAGA 3, *J. Geophys. Res.*, *98*(D9), 16,997–17,010, doi:10.1029/92JD02481.

Dentener, F. J., and P. J. Crutzen (1994), A three-dimensional model of the global ammonia cycle, *J. Atmos. Chem.*, *19*(4), 331–369, doi:10.1007/BF00694492.

Dixon, J. L. (2008), Macro and micro nutrient limitation of microbial productivity in oligotrophic subtropical atlantic waters, *Environ. Chem.*, *5*(2), 135–142.

Doney, S. C., I. Lima, R. A. Feely, D. M. Glover, K. Lindsay, N. Mahowald, J. K. Moore, and R. Wanninkhof (2009), Mechanisms governing interannual variability in upper-ocean inorganic carbon system and air-sea CO_2 fluxes: Physical climate and atmospheric dust, *Deep Sea Res. Part II*, *56*(8–10), 640–655, doi:10.1016/j.dsr2.2008.12.006.

Ducklow, H. W., and R. P. Harris (1993), Introduction to the JGOFS North Atlantic bloom experiment, *Deep Sea Res., Part II*, *40*(1–2), 1–8, doi:10.1016/0967-0645(93)90003-6.

Dunne, J. P., et al. (2012), GFDL's ESM2 global coupled climate–carbon Earth System Models. Part I: Physical formulation and baseline simulation characteristics, *J. Clim.*, *25*(19), 6646–6665, doi:10.1175/JCLI-D-11-00560.1.

Dunne, J. P., et al. (2013), GFDL's ESM2 global coupled climate-carbon Earth System Models. Part II: Carbon system formulation and baseline simulation characteristics, *J. Clim.*, *26*(7), 2247–2267, doi:10.1175/JCLI-D-12-00150.1.

Eppley, R. W., J. N. Rogers, and J. J. McCarthy (1969), Half-saturation constants for uptake of nitrate and ammonium by marine phytoplankton, *Limnol. Oceanogr.*, *14*, 912–920.

Facchini, M. C., et al. (2008), Important source of marine secondary organic aerosol from biogenic amines, *Environ. Sci. Technol.*, *42*(24), 9116–9121, doi:10.1021/es8018385.

Feng, Y., and J. E. Penner (2007), Global modeling of nitrate and ammonium: Interaction of aerosols and tropospheric chemistry, *J. Geophys. Res.*, *112*, D01304, doi:10.1029/2005JD006404.

Fernández, C., L. Farías, and M. E. Alcaman (2009), Primary production and nitrogen regeneration processes in surface waters of the Peruvian upwelling system, *Prog. Oceanogr.*, *83*(1-4), 159–168, doi:10.1016/j.pocean.2009.07.010.

Fisher, J. A., et al. (2011), Sources, distribution, and acidity of sulfate-ammonium aerosol in the Arctic in winter-spring, *Atmos. Environ.*, *45*, 7301–7318.

Fountoukis, C., and A. Nenes (2007), ISORROPIA II: A computationally efficient thermodynamic equilibrium model for K^+–Ca^{2+}–Mg^{2+}–NH_4^+–Na^+–SO_4^{2-}–NO_3^-–Cl^-–H_2O aerosols, *Atmos. Chem. Phys.*, *7*(17), 4639–4659, doi:10.5194/acp-7-4639-2007.

Fowler, D., et al. (2013), The global nitrogen cycle in the twenty-first century, *Philos. Trans. R. Soc. B*, *368*(1621), 1–13, doi:10.1098/rstb.2013.0164.

Fridlind, A. M., and M. Z. Jacobson (2000), A study of gas-aerosol equilibrium and aerosol pH in the remote marine boundary layer during the first aerosol characterization experiment (ACE 1), *J. Geophys. Res.*, *105*(D13), 17,325–17,340, doi:10.1029/2000JD900209.

Frost, B., and N. Franzen (1992), Grazing and iron limitation in the control of phytoplankton stock and nutrient concentration: A chemostat analogue of the Pacific Equatorial upwelling zone, *Mar. Ecol. Prog. Ser.*, *83*(2), 291–303.

Galloway, J. N., et al. (2004), Nitrogen cycles: Past, present, and future, *Biogeochemistry*, *70*(2), 153–226.

Garcia, H. E., R. A. Locarnini, T. P. Boyer, J. I. Antonov, O. K. Baranova, M. M. Zweng, J. R. Reagan, and D. R. Johnson (2014), *World Ocean Atlas 2013, Volume 4: Dissolved Inorganic Nutrients (Phosphate, Nitrate, Silicate)*, vol. 76, pp. 1–25, NOAA Atlas NESDIS, U.S. Department of Commerce, Asheville, N. C.

Gibb, S. W., R. F. C. Mantoura, and P. S. Liss (1999), Ocean-atmosphere exchange and atmospheric speciation of ammonia and methylamines in the region of the NW Arabian Sea, *Global Biogeochem. Cycles*, *13*(1), 161–178, doi:10.1029/98GB00743.

Griffies, S. J. (2012), Elements of the Modular Ocean Model (MOM): 2012 Release. GFDL Ocean Group Technical Report No. 7., Tech. Rep., NOAA/Geophysical Fluid Dynamics Laboratory. [Available at http://www.mom-ocean.org/web/docs.]

Gruber, N. (2004), The dynamics of the marine nitrogen cycle and its influence on atmospheric CO_2 variations, in *The Ocean Carbon Cycle and Climate*, edited by M. Follows and and T. Oguz, pp. 97–148, Springer, Netherlands, Dordrecht., doi:10.1007/978-1-4020-2087-2_4

Gruber, N. (2008), *The Marine Nitrogen Cycle: Overview and Challenges*, 2nd ed., pp. 1–50, Acad. Press, Waltham, Mass., doi:10.1016/B978-0-12-372522-6.00001-3.

Harrison, W., L. Harris, and B. Irwin (1996), The kinetics of nitrogen utilization in the oceanic mixed layer: Nitrate and ammonium interactions at nanomolar concentrations, *Limnol. Oceanogr.*, *41*(1), 16–32.

Holmes, R., B. Peterson, A. Zhulidov, V. Gordeev, P. Makkaveev, P. Stunzhas, L. Kosmenko, G. Köhler, and A. Shiklomanov (2001), Nutrient chemistry of the Ob' And Yenisey rivers, Siberia: Results from June 2000 expedition and evaluation of long-term data sets, *Mar. Chem.*, *75*(3), 219–227, doi:10.1016/S0304-4203(01)00038-X.

Huebert, B. J., T. Bates, P. B. Russell, G. Shi, Y. J. Kim, K. Kawamura, G. Carmichael, and T. Nakajima (2003), An overview of ACE-Asia: Strategies for quantifying the relationships between Asian aerosols and their climatic impacts, *J. Geophys. Res.*, *108*, 8633, doi:10.1029/2003JD003550.

Jaeglé, L., P. K. Quinn, T. S. Bates, B. Alexander, and J.-T. Lin (2011), Global distribution of sea salt aerosols: New constraints from in situ and remote sensing observations, *Atmos. Chem. Phys.*, *11*(7), 3137–3157, doi:10.5194/acp-11-3137-2011.

Jickells, T. D., S. D. Kelly, A. R. Baker, K. Biswas, P. F. Dennis, L. J. Spokes, M. Witt, and S. G. Yeatman (2003), Isotopic evidence for a marine ammonia source, *Geophys. Res. Lett.*, *30*, 1374, doi:10.1029/2002GL016728.

Johnson, M. T. (2010), A numerical scheme to calculate temperature and salinity dependent air-water transfer velocities for any gas, *Ocean Sci.*, *6*(4), 913–932, doi:10.5194/os-6-913-2010.

Johnson, M. T., P. S. Liss, T. G. Bell, T. J. Lesworth, A. R. Baker, A. J. Hind, T. D. Jickells, K. F. Biswas, E. M. S.Woodward, and S. W. Gibb (2008), Field observations of the ocean-atmosphere exchange of ammonia: Fundamental importance of temperature as revealed by a comparison of high and low latitudes, *Global Biogeochem. Cycles*, *22*, GB1019, doi:10.1029/2007GB003039.

Joubert, W. R., S. J. Thomalla, H. N. Waldron, M. I. Lucas, M. Boye, F. A. C. Le Moigne, F. Planchon, and S. Speich (2011), Nitrogen uptake by phytoplankton in the Atlantic sector of the Southern Ocean during late austral summer, *Biogeosciences*, *8*(10), 2947–2959, doi:10.5194/bg-8-2947-2011.

Keene, W. C., et al. (1989), An intercomparison of measurement systems for vapor and particulate phase concentrations of formic and acetic acids, *J. Geophys. Res.*, *94*(D5), 6457–6471, doi:10.1029/JD094iD05p06457.

Keene, W. C., M. S. Long, A. A. P. Pszenny, R. Sander, J. R. Maben, A. J. Wall, T. L. O'Halloran, A. Kerkweg, E. V. Fischer, and O. Schrems (2009), Latitudinal variation in the multiphase chemical processing of inorganic halogens and related species over the Eastern North and South Atlantic oceans, *Atmos. Chem. Phys.*, *9*(19), 7361–7385, doi:10.5194/acp-9-7361-2009.

Kitidis, V., G. Uher, R. C. Upstill-Goddard, R. F. C. Mantoura, G. Spyres, and E. M. S. Woodward (2006), Photochemical production of ammonium in the oligotrophic Cyprus Gyre (Eastern Mediterranean), *Biogeosciences*, *3*(4), 439–449, doi:10.5194/bg-3-439-2006.

Krishnamurti, T., B. Jha, J. Prospero, A. Jayaraman, and V. Ramanathan (1998), Aerosol and pollutant transport and their impact on radiative forcing over the tropical Indian Ocean during the January-February 1996 pre-INDOEX cruise, *Tellus B*, *50*(5), 521–542.

Kuypers, M. M. M., G. Lavik, D. Woebken, M. Schmid, B. M. Fuchs, R. Amann, B. B. Jørgensen, and M. S. M. Jetten (2005), Massive nitrogen loss from the Benguela upwelling system through anaerobic ammonium oxidation, *Proc. Natl. Acad. Sci.*, *102*(18), 6478–6483, doi:10.1073/pnas.0502088102.

Lamarque, J.-F., et al. (2010), Historical (1850–2000) gridded anthropogenic and biomass burning emissions of reactive gases and aerosols: Methodology and application, *Atmos. Chem. Phys.*, *10*(15), 7017–7039, doi:10.5194/acp-10-7017-2010.

Lana, A., et al. (2011), An updated climatology of surface dimethlysulfide concentrations and emission fluxes in the global ocean, *Global Biogeochem. Cycles*, *25*, GB1004, doi:10.1029/2010GB003850.

Legrand, M., F. Ducroz, D. Wagenbach, R. Mulvaney, and J. Hall (1998), Ammonium in coastal Antarctic aerosol and snow: Role of polar ocean and penguin emissions, *J. Geophys. Res.*, *103*(D9), 11,043–11,056, doi:10.1029/97JD01976.

Legrand, M., V. Gros, S. Preunkert, R. Sarda-Estève, A.-M. Thierry, G. Pépy, and B. Jourdain (2012), A reassessment of the budget of formic and acetic acids in the boundary layer at Dumont d'Urville (coastal Antarctica): The role of penguin emissions on the budget of several oxygenated volatile organic compounds, *J. Geophys. Res.*, *117*, D06308, doi:10.1029/2011JD017102.

Liss, P. S., and P. G. Slater (1974), Flux of gases across the air-sea interface, *Nature*, *247*(5438), 181–184, doi:10.1038/247181a0.

Liu, H., D. J. Jacob, I. Bey, and R. M. Yantosca (2001), Constraints from ^{210}Pb and ^{7}Be on wet deposition and transport in a global three-dimensional chemical tracer model driven by assimilated meteorological fields, *J. Geophys. Res.*, *106*, 12,109–12,128.

Luo, C., C. S. Zender, H. Bian, and S. Metzger (2007), Role of ammonia chemistry and coarse mode aerosols in global climatological inorganic aerosol distributions, *Atmos. Environ.*, *41*(12), 2510–2533, doi:10.1016/j.atmosenv.2006.11.030.

Milne, P. J., and R. G. Zika (1993), Amino acid nitrogen in atmospheric aerosols: Occurrence, sources and photochemical modification, *J. Atmos. Chem.*, *16*(4), 361–398, doi:10.1007/BF01032631.

Moore, J., S. C. Doney, J. A. Kleypas, D. M. Glover, and I. Y. Fung (2001), An intermediate complexity marine ecosystem model for the global domain, *Deep Sea Res., Part II*, *49*(1–3), 403–462, doi:10.1016/S0967-0645(01)00108-4.

Moore, J. K., S. C. Doney, and K. Lindsay (2004), Upper ocean ecosystem dynamics and iron cycling in a global three-dimensional model, *Global Biogeochem. Cycles*, *18*, GB4028, doi:10.1029/2004GB002220.

Morell, J. M., and J. E. Corredor (2001), Photomineralization of fluorescent dissolved organic matter in the Orinoco river plume: Estimation of ammonium release, *J. Geophys. Res.*, *106*(C8), 16,807–16,813, doi:10.1029/1999JC000268.

Murray, J. W., E. Johnson, and C. Garside (1995), A U.S. JGOFS process study in the Equatorial Pacific (EqPac): Introduction, *Deep Sea Res., Part II*, *42*(2–3), 275–293, doi:10.1016/0967-0645(95)00044-Q.

Nakamura, T., K. Matsumoto, and M. Uematsu (2005), Chemical characteristics of aerosols transported from Asia to the East China Sea: An evaluation of anthropogenic combined nitrogen deposition in autumn, *Atmos. Environ.*, *39*(9), 1749–1758, doi:10.1016/j.atmosenv.2004.11.037.

Nielsen, C. J., et al. (2011), Atmospheric Degradation of Amines (ADA). Summary report: Photo-oxidation of methylamine, dimethylamine and trimethylamine, Norsk Institutt for Luftforskning. [Available at http://www.nilu.no/Default.aspx?tabid=62&ctl=PublicationDetails&mid=764&publicationid=25495.]

Nightingale, P. D., P. S. Liss, and P. Schlosser (2000), Measurements of air-sea gas transfer during an open ocean algal bloom, *Geophys. Res. Lett.*, *27*(14), 2117–2120, doi:10.1029/2000GL011541.

Norman, M., and C. Leck (2005), Distribution of marine boundary layer ammonia over the Atlantic and Indian Oceans during the Aerosols99 cruise, *J. Geophys. Res.*, *110*, D16302, doi:10.1029/2005JD005866.

Paulot, F., D. J. Jacob, R. W. Pinder, J. O. Bash, K. Travis, and D. K. Henze (2014), Ammonia emissions in the United States, European Union, and China derived by high-resolution inversion of ammonium wet deposition data: Interpretation with a new agricultural emissions inventory (MASAGE_NH3), *J. Geophys. Res. Atmos.*, *119*, 4343–4364, doi:10.1002/2013JD021130.

Phinney, L., W. Richard Leaitch, U. Lohmann, H. Boudries, D. R. Worsnop, J. T. Jayne, D. Toom-Sauntry, M. Wadleigh, S. Sharma, and N. Shantz (2006), Characterization of the aerosol over the sub-Arctic North East Pacific Ocean, *Deep Sea Res., Part II*, *53*(20–22), 2410–2433, doi:10.1016/j.dsr2.2006.05.044.

Popova, E. E., M. A. Srokosz, and D. A. Smeed (2002), Real-time forecasting of biological and physical dynamics at the Iceland-Faeroes Front in June 2001, *Geophys. Res. Lett.*, *29*(4), 1055, doi:10.1029/2001GL013706.

Quinn, P. K., and T. S. Bates (2011), The case against climate regulation via oceanic phytoplankton sulphur emissions, *Nature*, *480*(7375), 51–56, doi:10.1038/nature10580.

Quinn, P. K., R. J. Charlson, and T. S. Bates (1988), Simultaneous observations of ammonia in the atmosphere and ocean, *Nature*, *335*(6188), 336–338, doi:10.1038/335336a0.

Quinn, P. K., T. S. Bates, J. E. Johnson, D. S. Covert, and R. J. Charlson (1990), Interactions between the sulfur and reduced nitrogen cycles over the central Pacific Ocean, *J. Geophys. Res.*, *95*(D10), 16,405–16,416, doi:10.1029/JD095iD10p16405.

Quinn, P. K., W. E. Asher, and R. J. Charlson (1992), Equilibria of the marine multiphase ammonia system, *J. Atmos. Chem.*, *14*(1–4), 11–30, doi:10.1007/BF00115219.

Quinn, P. K., K. J. Barrett, F. J. Dentener, F. Lipschultz, and K. D. Six (1996), Estimation of the air/sea exchange of ammonia for the North Atlantic basin, *Biogeochemistry*, *35*(1), 275–304, doi:10.2307/1469232.

Raes, F., T. Bates, F. McGovern, and M. Van Liedekerke (2000), The 2nd aerosol characterization experiment (ACE-2): general overview and main results, *Tellus B*, *52*(2), 111–125, doi:10.1034/j.1600-0889.2000.00124.x.

Rain-Franco, A., C. Muñoz, and C. Fernandez (2014), Ammonium production off Central Chile (36°S) by photodegradation of phytoplankton-derived and marine dissolved organic matter, *PLoS ONE*, *9*(6), e100224, doi:10.1371/journal.pone.0100224.

Riddick, S., U. Dragosits, T. Blackall, F. Daunt, S. Wanless, and M. Sutton (2012), The global distribution of ammonia emissions from seabird colonies, *Atmos. Environ.*, *55*, 319–327, doi:10.1016/j.atmosenv.2012.02.052.

Sarthou, G., A. R. Baker, J. Kramer, P. Laan, A. Laës, S. Ussher, E. P. Achterberg, H. J. de Baar, K. R. Timmermans, and S. Blain (2007), Influence of atmospheric inputs on the iron distribution in the subtropical north-east Atlantic Ocean, *Mar. Chem.*, *104*(3), 186–202.

Schlesinger, W. H., and A. E. Hartley (1992), A global budget for atmospheric NH_3, *Biogeochemistry*, *15*(3), 191–211.

Seitzinger, S., J. Harrison, E. Dumont, A. H. Beusen, and A. Bouwman (2005), Sources and delivery of carbon, nitrogen, and phosphorus to the coastal zone: An overview of global nutrient export from watersheds (NEWS) models and their application, *Global Biogeochem. Cycles*, *19*, GB4S01, doi:10.1029/2005GB002606.

Shiomoto, A., K. Sasaki, T. Shimoda, and S. Matsumura (1994), Kinetics of nitrate and ammonium uptake by the natural populations of marine phytoplankton in the surface water of the Oyashio region during spring and summer, *J. Oceanogr.*, *50*(5), 515–529.

Smith, J. M., F. P. Chavez, and C. A. Francis (2014), Ammonium uptake by phytoplankton regulates nitrification in the sunlit ocean, *PLoS ONE*, *9*(9), e108173, doi:10.1371/journal.pone.0108173.

Smith, S. D. (1980), Wind stress and heat flux over the ocean in gale force winds, *J. Phys. Oceanogr.*, *10*(5), 709–726, doi:10.1175/1520-0485(1980)010<0709:WSAHFO>2.0.CO;2.

Smith, S. L., L. A. Codispoti, J. M. Morrison, and R. T. Barber (1998), The 1994–1996 Arabian Sea expedition: An integrated, interdisciplinary investigation of the response of the northwestern Indian Ocean to monsoonal forcing, *Deep Sea Res., Part II*, *45*(10-11), 1905–1915, doi:10.1016/S0967-0645(98)00058-7.

Smith, W. O., Jr., R. F. Anderson, J. Keith Moore, L. A. Codispoti, and J. M. Morrison (2000), The US Southern Ocean joint global ocean flux study: An introduction to AESOPS, *Deep Sea Res., Part II*, *47*(15-16), 3073–3093, doi:10.1016/S0967-0645(00)00059-X.

Solorzano, L., et al. (1969), Determination of ammonia in natural waters by the phenolhypochlorite method, *Limnol. Oceanogr*, *14*(5), 799–801.

Stock, C. A., J. P. Dunne, and J. G. John (2014a), Global-scale carbon and energy flows through the marine planktonic food web: An analysis with a coupled physical-biological model, *Prog. Oceanogr.*, *120*, 1–28, doi:10.1016/j.pocean.2013.07.001.

Stock, C. A., J. P. Dunne, and J. G. John (2014b), Drivers of trophic amplification of ocean productivity trends in a changing climate, *Biogeosciences*, *11*(24), 7125–7135, doi:10.5194/bg-11-7125-2014.

Streets, D. G., et al. (2003), An inventory of gaseous and primary aerosol emissions in Asia in the year 2000, *J. Geophys. Res.*, *108*(D21), 8809, doi:10.1029/2002JD003093.

Sutka, R. L., N. E. Ostrom, P. H. Ostrom, and M. S. Phanikumar (2004), Stable nitrogen isotope dynamics of dissolved nitrate in a transect from the north Pacific subtropical gyre to the eastern tropical North Pacific, *Geochim. Cosmochim. Acta*, *68*(3), 517–527, doi:10.1016/S0016-7037(03)00483-6.

Sutton, M. A., J. W. Erisman, F. Dentener, and D. Möller (2008), Ammonia in the environment: From ancient times to the present, *Environ. Pollut.*, *156*(3), 583–604, doi:10.1016/j.envpol.2008.03.013.

Sutton, M. A., et al. (2013), Towards a climate-dependent paradigm of ammonia emission and deposition, *Philos. Trans. R. Soc. B*, *368*(1621), 20130166, doi:10.1098/rstb.2013.0166.

Uematsu, M., M. Toratani, M. Kajino, Y. Narita, Y. Senga, and T. Kimoto (2004), Enhancement of primary productivity in the western North Pacific caused by the eruption of the Miyake-jima Volcano, *Geophys. Res. Lett.*, *31*, L06106, doi:10.1029/2003GL018790.

van der Werf, G. R., J. T. Randerson, L. Giglio, G. J. Collatz, M. Mu, P. S. Kasibhatla, D. C. Morton, R. S. DeFries, Y. Jin, and T. T. van Leeuwen (2010), Global fire emissions and the contribution of deforestation, savanna, forest, agricultural, and peat fires (1997–2009), *Atmos. Chem. Phys.*, *10*(23), 11,707–11,735.

Wang, J., A. A. Hoffmann, R. J. Park, D. J. Jacob, and S. T. Martin (2008), Global distribution of solid and aqueous sulfate aerosols: Effect of the hysteresis of particle phase transitions, *J. Geophys. Res.*, *113*, D11206, doi:10.1029/2007JD009367.

Wang, Q., et al. (2011), Sources of carbonaceous aerosols and deposited black carbon in the Arctic in winter-spring: Implications for radiative forcing, *Atmos. Chem. Phys.*, *11*(23), 12,453–12,473.

Ward, B., R. J. Olson, and M. J. Perry (1982), Microbial nitrification rates in the primary nitrite maximum off Southern California, *Deep Sea Res., Part II*, *29*(2), 247–255.

Whitledge, T. E., S. Malloy, C. Patton, and C. Wirick (1981), Automated nutrient analyses in seawater, Brookhaven National Lab., Upton, New York.

Wood, R., et al. (2011), The VAMOS ocean-cloud-atmosphere-land study regional experiment (VOCALS-REx): Goals, platforms, and field operations, *Atmos. Chem. Phys.*, *11*(2), 627–654, doi:10.5194/acp-11-627-2011.

Xie, H., S. Bélanger, G. Song, R. Benner, A. Taalba, M. Blais, J.-É. Tremblay, and M. Babin (2012), Photoproduction of ammonium in the southeastern beaufort sea and its biogeochemical implications, *Biogeosciences*, *9*(8), 3047–3061, doi:10.5194/bg-9-3047-2012.

Yoneyama, K., C. Zhang, and C. N. Long (2013), Tracking pulses of the Madden-Julian oscillation, *Bull. Am. Meteorol. Soc.*, *94*, 1871–1891, doi:10.1175/BAMS-D-12-00157.1.

Yool, A., A. P. Martin, C. Fernández, and D. R. Clark (2007), The significance of nitrification for oceanic new production, *Nature*, *447*(7147), 999–1002, doi:10.1038/nature05885.

Zhang, Q., and C. Anastasio (2003), Conversion of fogwater and aerosol organic nitrogen to ammonium, nitrate, and NO_x during exposure to simulated sunlight and ozone, *Environ. Sci. Technol.*, *37*(16), 3522–3530, doi:10.1021/es034114x.

Zhang, R., A. Khalizov, L. Wang, M. Hu, and W. Xu (2011), Nucleation and growth of nanoparticles in the atmosphere, *Chem. Rev.*, *112*(3), 1957–2011.

Zorn, S. R., F. Drewnick, M. Schott, T. Hoffmann, and S. Borrmann (2008), Characterization of the South Atlantic marine boundary layer aerosol using an aerodyne aerosol mass spectrometer, *Atmos. Chem. Phys.*, *8*(16), 4711–4728, doi:10.5194/acp-8-4711-2008.